Supporting Information for *Nano Letters* DOI: http://dx.doi.org/10.1021/nl202782q

Crystal Face-Dependent Nanopiezotronics of an Obliquely Aligned InN Nanorod Array

*Nai-Jen Ku[1], Jun-Han Huang[1], Chao-Hung Wang[1], Hsin-Chiao Fang[1] and Chuan-Pu Liu[1,2,3,4]**

[1]Department of Materials Science and Engineering, National Cheng Kung University, Tainan 701, Taiwan

[2]Center for Micro/Nano Science and Technology, National Cheng Kung University, Tainan 701, Taiwan

[3]Center for Energy Technology and Strategy, National Cheng Kung University, Tainan 701, Taiwan

[4]Advanced Optoelectronic Technology Center, National Cheng Kung University, Tainan 701, Taiwan

*Corresponding author. E-mail: cpliu@mail.ncku.edu.tw

InN materials have attracted a lot of attention for application in nanogenerators and piezotronics due to their relatively large piezoelectric constant. However, the surface-dependent electrical properties of quantized surface electron accumulation layers have rarely been studied. This study uses an obliquely aligned InN nanorod array to explore crystal-surface-dependent nanopiezotronic properties. Researchers have recently used glancing angle deposition to fabricate one-dimensional obliquely aligned nanostructures for applications involving energy-related devices and sensors. This approach makes it possible for devices such as nanogenerators or nanopiezotronics to utilize the elastic deformation of one-dimensional piezoelectric nanorods by simply applying a normal force. Many other devices, such as thermoelectric cells, can be devised by incorporating these nanostructures. This supporting information provides detailed information on the methods and equivalent circuit used for nanopiezotronic measurements, extensive material characterization, and the validation of theoretical models.

Through the orientation control of obliquely aligned InN nanorods, the effects of the quantized electron surface accumulation layer on the electron transport properties are investigated by conductive atomic force microscopy (C-AFM). The InN nanorod sample for C-AFM measurements was grown on a highly doped Si(111) substrate, as shown in the schematic diagram of Figure 1S(a). The prepared sample was attached to a metal electrode using silver paint to create a Schottky contact. For the C-AFM experiments, a Seiko SPA-400 atomic force microscope was operated in contact mode with a Pt/Ir-coated Si conductive probe used as the grounded electrode. The conductive AFM tips employed (provided by nanoScience Instruments) had a typical uncoated tip radius of 5-6 nm and a cone angle of about 25°. A conductive Pt/Ir coating was applied to both sides of the cantilever, resulting in a tip radius of less than 30 nm. Therefore, the space between two adjacent InN nanorods was sufficiently large for the force-dependent piezotronic measurement and for the influence of the interface to be neglected. An equivalent circuit diagram is shown in Figure 1S(b). Because the electron affinity of n-type InN (5.8 eV) is smaller than that of the Pt/Ir tip (6.1 eV), a Schottky junction formed at the Pr/InN interface. The detection range of the current was varied from 0.1 to 100 nA in saturation. Due to the sharp and asymmetric current increase between the top and sidewall planes, shown in Figure 3(c), the current contribution from the contact area difference between the (0002) plane and $(\bar{1}102)$ plane was relatively minor compared to the influence of the Schottky barrier height (SBH) change.

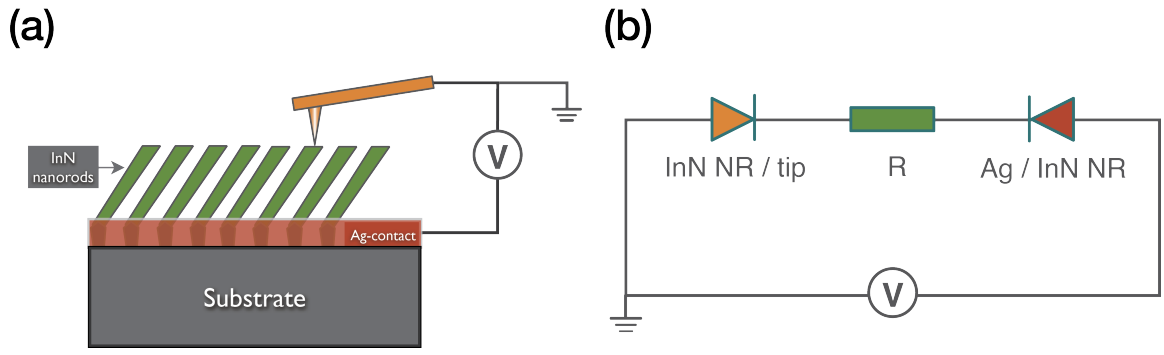

Figure 1S. Schematic diagrams showing (a) experimental arrangement and (b) equivalent circuit for an InN nanorod at a negative bias with respect to the tip. "*R*" represents the resistance of the InN nanorod.

The μ-Raman spectrum was acquired with a LabRam HR confocal microprobe Raman system (Horiba Jobin-Yvon) using a He-Ne laser with an excitation of 632.8 nm. The μ-Raman spectrum in Figure 2S is characterized by a very narrow E_2^h phonon peak at 488 cm^{-1} (full width at half maximum (FWHM) = 4.9 ± 0.1 cm^{-1}), confirming that the InN nanorods were strain-free with high crystalline quality. The μ-Raman spectrum also shows a broad band centered at 435 cm^{-1}, which can be attributed to the low branch of longitudinal optical modes coupled to an electron plasma mode (PLP^-). This broad band suggests the existence of a high concentration ($10^{19} \sim 10^{20}$ cm^{-3}) of degenerated electrons present at the surfaces.

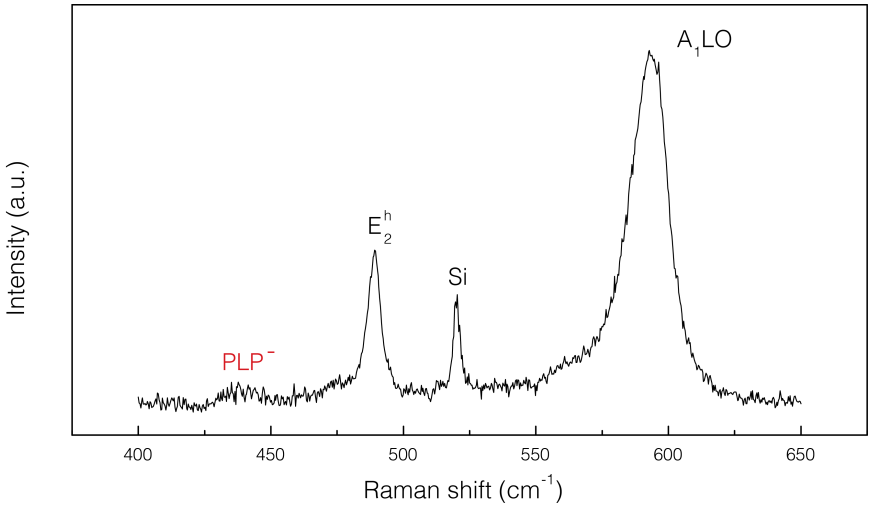

Figure 2S. Room-temperature μ-Raman spectrum of obliquely aligned InN nanorods, showing a very narrow E_2^h phonon peak at 488 cm^{-1} and an A_1LO mode at 593 cm^{-1}. There is a plasmon-longitudinal optical phonon coupled (PLP^-) mode at 435 cm^{-1}.

Schottky junctions form at the interfaces between the Pt/Ir tip and InN nanorod surfaces and can be described by the thermionic-emission-diffusion (TED) model. The TED theory attempts to explain the I-V behavior of Schottky diodes in contact with the (0002) and ($\bar{1}$102) planes of an InN nanorod. Assuming that the SBH, ϕ_s, is larger than kT, the current density is given as: [1-3]

$$J_{TED} = A^{**}T^2 \exp\left(-\frac{\phi_s}{kT}\right)\exp\left(\frac{q\phi_f}{kT}\right)$$

$$\phi_f = \sqrt{\frac{q\mathcal{E}_m}{4\pi\varepsilon_s}}, \quad \mathcal{E}_m = \sqrt{\frac{2qN_D^+}{\varepsilon_s}\left(V + V_{bi} - \frac{kT}{q}\right)} \qquad (1S)$$

where A^{**} is the effective Richardson constant, q is the electron charge, k is the Boltzmann constant, f_f is the image force correction, N_D^+ is the donor concentration, V is the applied voltage, V_{bi} is the build-in potential at the barrier, and ε_s is the permittivity of InN. Figure 3S verifies the TED theory model by comparing the experimental I-V curves with a theoretical fitting obtained from a plot of the natural logarithm of the current density as a function of $V^{1/4}$. The almost perfect fitting proves that electron transport through the (0002) and ($\bar{1}$102) planes by the classic TED model. Of note, the current fluctuates at certain biases (marked by arrows), implying the existence of quantum subband energy states in the electron accumulation layer.

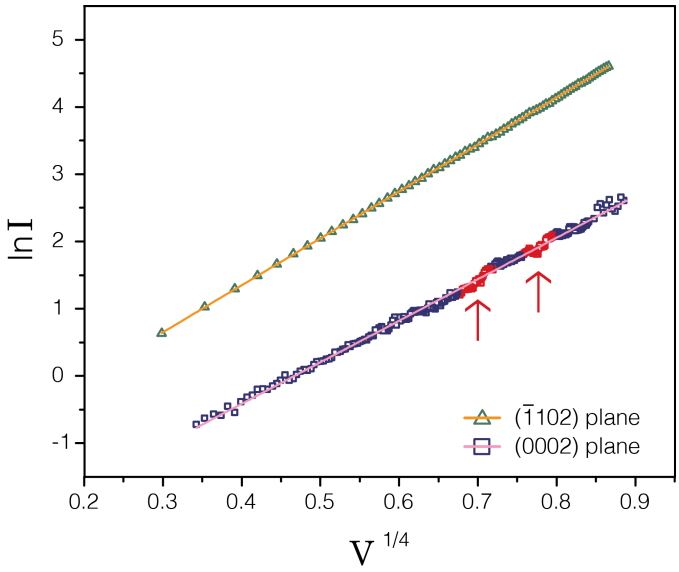

Figure 3S. Plot of ln *I* as a function of $V^{1/4}$ for the curves in Figure 2(a) with the best fitting obtained using Equation (1S).

By using the one-electron potential and Poisson's equation[4] to describe the band bending in the space-charge region, the energy difference between pairs of subbands (ΔE_n) in the surface electron accumulation layer of InN was calculated; the results are shown in Figure 4S. From the experimental results shown in Figure 2(d), the energy difference ($V_{1,2}^{(0002)} = 207\,\text{mV}$) measured for the (0002) plane corresponds to a surface state density (N_{ss}) of about ~2×10^{13} cm^{-2}, which agrees with the calculated value[4] for a typical unintentionally doped MBE-grown InN (N_{ss}=1.6×10^{13} cm^{-2}). For the $(\bar{1}102)$ plane, the energy differences of $V_{1,2}^{(\bar{1}102)} = 102\,\text{mV}$ and $V_{2,3}^{(\bar{1}102)} = 161\,\text{mV}$ correspond to a surface state density ranging from N_{ss}=1×10^{13} cm^{-2} to N_{ss}=5×10^{13} cm^{-2}, which does not agree with the calculated values.[4] This discrepancy may be due to the uncertainty in the determination of the local minimum using d^2I/dV^2 for $V_1^{(\bar{1}102)} = 172\,\text{mV}$ in Figure 2(d) or some perturbations due to tip-induced band bending or surface Fermi-level pinning at surface defects.[4]

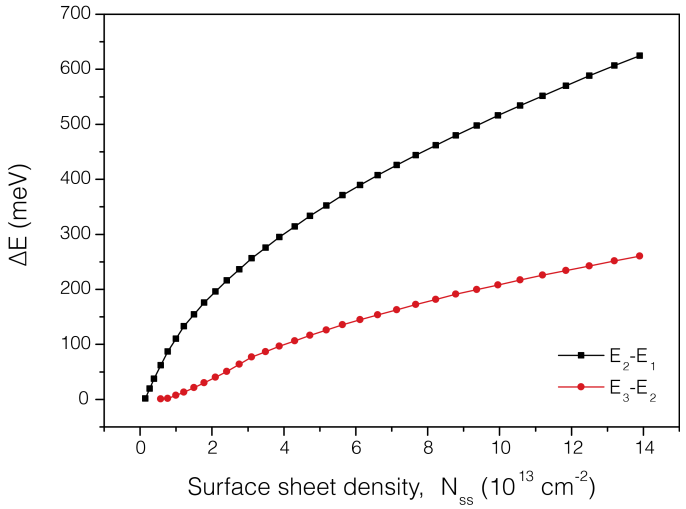

Figure 4S. Inter-subband energy difference, ΔE, as a function of surface sheet density (N_{ss}) obtained from theoretical calculations[4] for a bulk InN sample with a carrier density of 2.5×10^{18} cm^{-3}.

Figure 5S verifies the I-V curves shown in Figure 4(a) for various applied forces with the TED theory by plotting ln$I$ as a function of $V^{1/4}$. Perfect linear fitting is obtained in the high-resistance region ($V<V_{th}$).

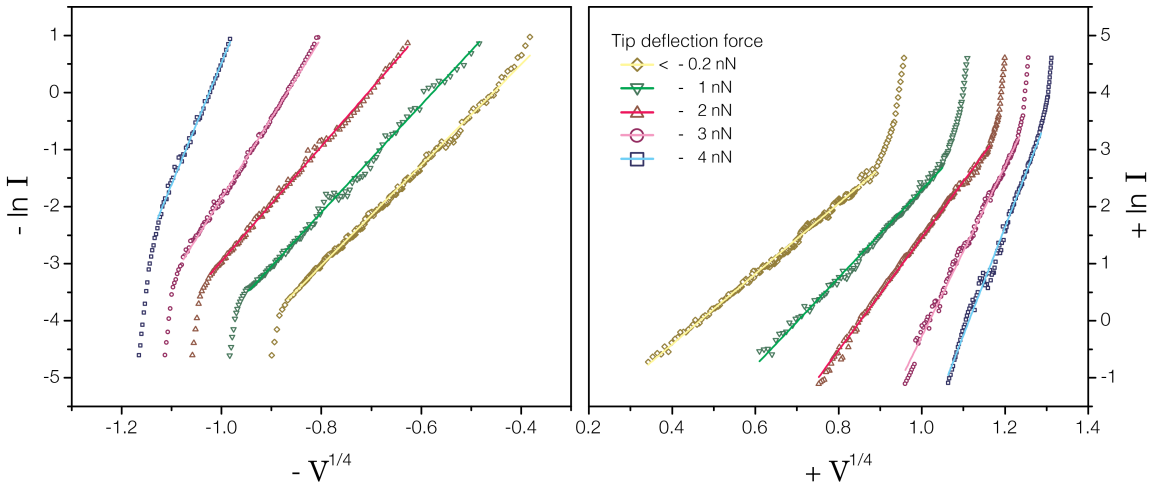

Figure 5S. Plot of ln$I$ as a function of $V^{1/4}$ for the I-V curves in Figure 4(a) with fitting obtained from TED theory in the high-resistance region according to Equation (1S).

SUPPORTING REFERENCES

(1) Zhou, J.; Fei, P.; Gu, Y.; Mai, W.; Gao, Y.; Yang, R.; Bao, G.; Wang, Z. L., *Nano Lett*. **2008,** *8* (11), 3973-3977.

(2) Zhou, J.; Gu, Y.; Fei, P.; Mai, W.; Gao, Y.; Yang, R.; Bao, G.; Wang, Z. L., *Nano Lett*. **2008,** *8* (9), 3035-3040.

(3) Sze, S. M.; Ng, K. K., *Physics of Semiconductor Devices*. 3rd ed.; Wiley-Interscience: Hoboken, New Jersey, 2007.

(4) King, P. D. C.; Veal, T. D.; McConville, C. F., *Phys. Rev. B* **2008,** *77* (12), 125305.